Fabrication and efficiency measurement of a multilayer-coated ion-beam-etched laminar grating for extreme ultraviolet region

Hui Lin (林 慧)[1*], Lichao Zhang (张立超)[2], Chunshui Jin (金春水)[2], Hongjun Zhou (周洪军)[3], and Tonglin Huo (霍同林)[3]

[1]*State Key Laboratory of Precision Measurement Technology and Instruments, Department of Precision Instruments, Tsinghua University, Beijing 100084*

[2]*State Key Lab of Applied Optics, Changchun Institute of Optics and Fine Mechanics and Physics, Chinese Academy of Sciences, Changchun 130022*

[3]*National Synchrotron Radiation Laboratory, University of Science and Technology of China, Hefei 230029*

[*]*E-mail: hui_lin00@mails.tsinghua.edu.cn*

Received August 18, 2008

We fabricate and measure a multilayer-coated ion-beam-etched laminar grating for the extreme ultraviolet wavelength region. The fabrication process is carefully controlled so that the grating groove and multilayer-coating parameters well meet the design targets. At an incident angle of 10°, the peak diffraction efficiency of the +1st order is 20.6% at 14.56 nm and that of the −1st order is 22.1% at 14.65 nm, both close to the theoretical limits.

OCIS codes: 050.1950, 120.4610, 310.1620, 340.7480.
doi: 10.3788/COL20090703.0180.

In the extreme ultraviolet (EUV) wavelength region, the near-normal-incidence diffraction efficiency of a reflection grating can be greatly enhanced by multilayer coating. As the operating wavelength is much less than the grating period, the scalar theory is valid for this region. The diffraction efficiency can be represented as the product of the multilayer reflectivity and the grating groove efficiency (efficiency of a perfectly conducting grating). Theoretically, a blazed grating with triangular groove shape has near 100% groove efficiency in a desired order[1]. By use of ion-beam etching technique, we have fabricated a blazed grating sample with $\sim 60\%$ groove efficiency and $\sim 36\%$ diffraction efficiency after multilayer coating[2]. A laminar grating with rectangular groove shape is not comparable with the blazed one in efficiency, because it has only a maximum groove efficiency of 40.5% in both of the +1st and −1st orders[1]. However, it does not mean that laminar gratings are useless in practice. On the contrary, laminar gratings are more applicable than blazed gratings due to the two reasons below. Firstly, it is simpler and more convenient to get a regular and uniform rectangular shape than a triangular one, especially for fabricating gratings of large sizes. Secondly, in order to reduce the reflection loss, concave gratings that gather both dispersion and focus functions are preferred for EUV spectrometers. It is difficult to fabricate blazed gratings on concave substrates by ion beam etching, because the required grazing-incidence ion beam cannot reach the substrate center[3]. In contrast, laminar gratings do not encounter such a problem, for the ion beam is normal to the substrate. As a result, laminar gratings have been adopted in most EUV spectral applications to date[4−7]. The highest measured efficiency of a multilayer-coated ion-beam-etched laminar grating, reported by Kowalski *et al.* in 1997, is $\sim 16\%$ in the −1st order at a wavelength of 15.12 nm and an incidence angle of 10°[8].

In this letter, we report our study of a Mo/Si multilayer-coated ion-beam-etched laminar grating. By precisely controlling the fabrication process, we made a grating sample whose groove and multilayer-coating parameters were close to design. The measured peak diffraction efficiency is 22.1%, which is close to the theoretical limit.

The grating sample was designed for the ±1st orders whose peak wavelength is $\sim$ 14.5 nm at 10° incidence. The groove density is 2400 lines/mm. To completely suppress the zeroth order and get maximum ±1st-order efficiency[1], the groove depth is designed to be 3.68 nm (about one fourth of the peak wavelength), and the duty cycle (the ratio of ridge width to period) is 0.5. Surface roughness can cause stray light, so its root-mean-square (rms) value must be less than 1 nm.

The grating sample was fabricated on a finely polished fused silica substrate of 30 × 30 (mm) in area and 1 mm in thickness. We first formed a rectangular-shape photoresist grating mask by following the holographic exposure-development steps. With a development monitoring technique[9], the duty cycle of the photoresist mask was controlled to be $\sim$0.5. Then the square wave pattern was transferred into the substrate by argon ion beam etching. To precisely control the groove depth by the etching time, we used an ion energy of 300 eV and an ion beam current density of 0.25 mA/cm^2 to lower the etching rate. The etching process lasted for 1 min.

Atomic force microscope (AFM) was used to measure the grating contour. Six locations in or around the sample center were measured. A typical AFM image is shown in Fig. 1(a). We used the algorithm introduced in Ref. [10] to deduce the grating parameters from the AFM

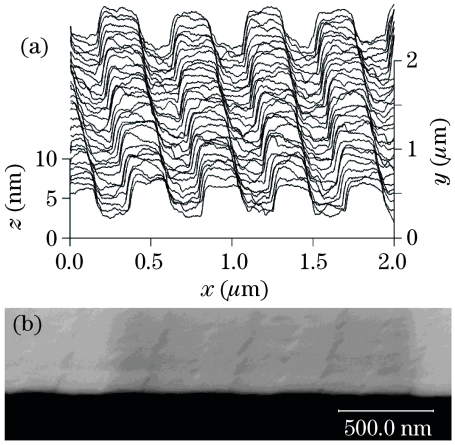

Fig. 1. Measured groove contour of the bare laminar grating sample. (a) AFM; (b) SEM.

Table 1. Designed and Measured Parameter Values of the Grating Sample

Parameter	Designed	Measured
Groove Density (lines/mm)	2400	2401 ± 1
Groove Depth (nm)	3.68	3.61 ± 0.12
Duty Cycle	0.50	0.48 ± 0.02
Roughness (nm)	< 1.0	0.55 ± 0.09

data. The groove depth was determined by the two peaks that represented the top and bottom of the grooves in the height histogram. The roughness was calculated by integrating the power spectral density over the range of $2 - 40\ \mu\text{m}^{-1}$. The duty cycle inferred from AFM data was a little larger than the actual value due to the convolution effect of the probe tip, so we determined it by scanning electronic microscope (SEM) measurement (Fig. 1(b)). The groove density was obtained by measuring the autocollimation diffraction angle of the -1st order at a wavelength of 632.8 nm. All the measured grating parameters are listed in Table 1, from which we find that the parameters well meet our design goal.

The multilayer coating composed of 40 periods of Mo/Si layer pairs was deposited onto the bare grating by ion-beam sputtering. The thickness of each layer pair (the period) was 7.6 nm and the ratio of the Mo thickness to the period was 0.4 so as to achieve the maximum reflectivity at a wavelength of 14.5 nm at 10° incidence. To evaluate the multilayer reflectivity individually, a witness flat layer of fused silica was coated simultaneously with the grating.

Efficiency measurements were made at the Spectral Radiation Standard and Metrology Beamline (U26) of the National Synchrotron Radiation Laboratory of China. The beamline was equipped with a scanning monochrometer that uses a spherical grating with spectral resolution ($\lambda/\Delta\lambda$) of ~ 192. To suppress the signal of higher harmonics, a filter made of silicon nitride was mounted after the monochrometer. We calibrated the wavelength scale of the monochrometer by measuring the Si L absorption edge of the filter. The sample was measured in a reflectometer which allowed the sample holder and the photodiode detector to move in several degrees of freedom. The incident radiation was about 80% s-polarization (electric vector parallel to the groove), and the spot size on the grating was $\sim 3 \times 1$ (mm).

We firstly measured the reflectivity of the witness flat layer at an incident angle of 10°. The detector was fixed to receive the reflected radiation while the monochrometer scanned the wavelength from 13.0 to 16.5 nm. The peak reflectivity was 62% and occurred at 14.52 nm.

We then measured the diffraction efficiency of the grating sample. A slit of about 0.8-mm width was mounted in front of the detector to resolve diffraction orders. We fixed the incident angle to 10°, and let the detector scan the diffraction angular spectra at wavelengths in increments of 0.045 nm from 13.71 to 15.24 nm. We measured the incident beam intensity at the beginning and the end of the 35-scan sequence, and observed that the incident beam intensity at the end was $\sim 8\%$ larger than that at the beginning. The incident beam intensity for each angular scan was obtained by linear interpolation of these two values with respect to the measurement time. Considering the drift of the incident beam intensity, we estimate that the relative deviation of diffraction efficiency measurement results is $\sim 10\%$.

Figure 2 shows the diffraction efficiencies of the $\pm$1st orders versus wavelengths. The peak efficiency of the -1st order is 22.1% at 14.65 nm and that of the $+1$st order is 20.6% at 14.56 nm. Based on the measured reflectivity of the witness flat layer, we infer that the peak groove efficiency is 35.6% for the -1st order and 33.2% for the $+1$st order, which are close to the theoretical limit of 40.5%. There is a small wavelength separation of 0.09 nm between the $\pm$1st orders, which is consistent with those observed in the previous work[11].

The high $\pm$1st-order efficiencies are accompanied by the good suppression of the other diffraction orders. Figure 3 illustrates the angular spectrum of diffraction efficiency measured at the peak wavelength of 14.65 nm for the -1st order. The efficiencies of the 0th, $\pm$2nd orders are $\sim 2\%$ each, which are only one tenth of the -1st-order peak efficiency. The stray light between diffraction orders is much weaker than the diffracted beams, owing to low roughness of the grating profile.

The high efficiency result is mainly due to our careful control of the fabrication process. Firstly the groove depth and the duty cycle of the sample were carefully controlled to meet the design target. We used a code based on the differential theory[12] to analyze the influence of the grating parameters on the groove efficiency. The

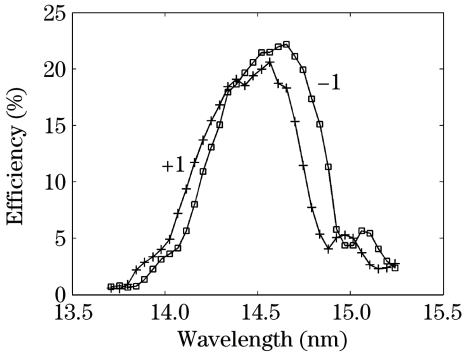

Fig. 2. Measured $\pm$1st-order diffraction efficiencies versus wavelength at an incident angle of 10°. Squares: -1st order; crosses: $+1$st order.

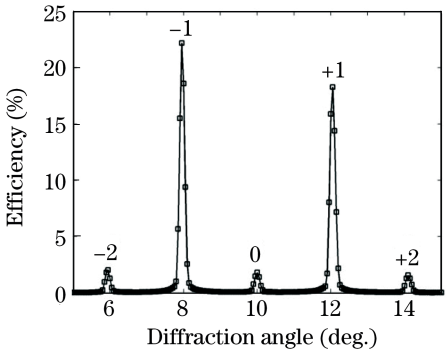

Fig. 3. Diffraction efficiency angular spectrum of the Mo/Si multilayer-coated laminar grating at a 10° incident angle and a 14.65-nm wavelength.

ideal rectangular shape was considered in calculation, because the groove of a laminar grating is shallow, and the inclined sidewall phenomenon[13] is not significant. The calculated results show that the groove depth should be $3.3 - 4.1$ nm and the duty cycle should be $0.42 - 0.58$ so as to reach 90% of the groove efficiency limit (40.5%) at 14.55 nm. Our sample satisfies such required precision. In addition, the theoretical groove efficiency is 39.7% by using the measured parameters shown in Table 1. The discrepancy between the measured groove efficiency (35.6%) and the theoretical prediction (39.7%) mainly results from the irregularities of the groove shape, such as the fluctuations at the top and bottom of the grooves. Secondly, the Mo/Si multilayer coating was precisely controlled. The peak reflectivity is 62%, which has approached the theoretical limit of 73%. The high reflectivity is attributed primarily to the low roughness of the substrate and the low inter-diffusion of the adjacent layers.

In conclusion, we succeed in fabricating a high-efficiency multilayer-coated ion-beam-etched laminar grating for use in the EUV wavelength region. By carefully controlling the fabrication process, we assured that the grating groove parameters and the multilayer coating were precisely on targets. The peak efficiency of the grating sample achieves 22.1% in the −1st order (35.6% groove efficiency times 62% multilayer reflectivity), which is close to the theoretical limit of $\sim$ 29% (40.5% groove efficiency limit times 73% multilayer reflectivity limit). In the future, we expect to fabricate laminar gratings on concave substrates with larger size in preparation for use in EUV spectrometers.

We thank Shu Pei of the State Key Laboratory of Applied Optics of China for AFM measurements and Wenyan Yang of Tsinghua University for SEM measurements. This work was supported by the National Natural Science Foundation of China (No. 60678034) and an internal fund of the State Key Laboratory of Applied Optics of China.

References

1. E. G. Loewen, M. Nevière, and D. Maystre, J. Opt. Soc. Am. **68,** 496 (1978).
2. H. Lin, L. Zhang, L. Li, C. Jin, H. Zhou, and T. Huo, Opt. Lett. **33,** 485 (2008).
3. Q. Zhou, L. Li, and L. Zeng, Proc. SPIE **6832,** 68320W (2007).
4. L. Yuan, Z. Fan, G. Yin, K. Yi, J. Shao, M. Cui, L. Liu, J. Miao, G. Chen, and X. Shen, Acta Opt. Sin. (in Chinese) **14,** 642 (1994).
5. M. P. Kowalski, T. W. Barbee, Jr., K. F. Heidemann, H. Gursky, J. C. Rife, W. R. Hunter, G. G. Fritz, and R. G. Cruddace, Appl. Opt. **38,** 6487 (1999).
6. J. F. Seely, C. M. Brown, D. L. Windt, S. Donguy, and B. Kjornrattanawanich, Appl. Opt. **43,** 1463 (2004).
7. T. Imazono, M. Ishino, M. Koike, H. Sasai, and K. Sano, Appl. Opt. **46,** 7054 (2007).
8. M. P. Kowalski, R. G. Cruddace, J. F. Seely, J. C. Rife, K. F. Heidemann, U. Heinzmann, U. Kleineberg, K. Osterried, D. Menke, and W. R. Hunter, Opt. Lett. **22,** 834 (1997).
9. L. Li, M. Xu, G. I. Stegeman, and C. T. Seaton, Proc. SPIE **835,** 72 (1987).
10. M. P. Kowalski, W. R. Hunter, and T. W. Barbee, Jr., Appl. Opt. **45,** 305 (2006).
11. L. I. Goray and J. F. Seely, Proc. SPIE **5900,** 59000C (2005).
12. M. Nevière, J. Opt. Soc. Am. A **8,** 1468 (1991).
13. X. Meng and L. Li, Acta Opt. Sin. (in Chinese) **28,** 189 (2008).